

# Tomographic Constraints on High-Energy Neutrinos of Hadronuclear Origin

Shin'ichiro Ando, Irene Tamborra, and Fabio Zandanel

GRAPPA Institute, University of Amsterdam, 1098 XH Amsterdam, The Netherlands

(Dated: September 14, 2015; revised October 22, 2015)

Mounting evidence suggests that the TeV–PeV neutrino flux detected by the IceCube telescope has mainly an extragalactic origin. If such neutrinos are primarily produced by a single class of astrophysical sources via hadronuclear ( $pp$ ) interactions, a similar flux of gamma-ray photons is expected. For the first time, we employ *tomographic constraints* to pinpoint the origin of the IceCube neutrino events by analyzing recent measurements of the cross correlation between the distribution of GeV gamma rays, detected by the Fermi satellite, and several galaxy catalogs in different redshift ranges. We find that the corresponding bounds on the neutrino luminosity density are up to one order of magnitude tighter than those obtained by using only the spectrum of the gamma-ray background, especially for sources with mild redshift evolution. In particular, our method excludes any hadronuclear source with a spectrum softer than  $E^{-2.1}$  as a main component of the neutrino background, if its evolution is slower than  $(1+z)^3$ . Starburst galaxies, if able to accelerate and confine cosmic rays efficiently, satisfy both spectral and tomographic constraints.

PACS numbers: 95.85.Pw, 95.85.Ry, 98.70.Rz, 98.70.Vc

*Introduction.*—The discovery of the PeV neutrinos by IceCube [1, 2] has launched the era of high-energy neutrino astronomy. The current data set is compatible with a flux in excess with respect to the atmospheric background, with an isotropic allocation of events on the celestial sphere and flavor equipartition [1–6]. Due to the current low statistics, the origin of the high-energy IceCube events is not yet known, but an extragalactic and mostly diffuse origin appears to be favored [7, 8].

The high-energy neutrino production from cosmic accelerators has been subject of a cascade of theoretical studies, especially after the IceCube results were announced [7, 8]. Many papers discuss the neutrino emission from one specific source class by adopting a model-dependent approach, for active galactic nuclei (AGNs) [9–18], star-forming galaxies [19–28], gamma-ray bursts [29–36], galaxy clusters [37–40], and dark matter decays [41–45].

Alternatively, a more generic approach focuses on the phenomenological aspects of the potential sources. For example, assuming photomeson production ( $p\gamma$ ) of neutrinos, Ref. [46] obtained constraints on the source size and magnetic field strength needed to match the IceCube flux. Reference [47] hypothesized that the TeV–PeV neutrinos were generated via hadronuclear interactions ( $pp$ ) and concluded that the cosmic ray spectrum of the dominant neutrino sources should be harder than  $E^{-2.2}$ . This is because the associated gamma-ray spectrum will extend down to GeV energies, where the flux of the isotropic gamma-ray background (IGRB) measured with the Fermi Large Area Telescope (LAT) [48] cannot be overshot. The connection with sources of ultrahigh-energy cosmic rays has also been considered [49–51].

In this *Letter*, we complement the existing model-independent investigations of  $pp$  neutrino sources by proposing an entirely new method: *Tomographic constraints*, up to now adopted in studying IGRB sources.

We base this approach on the measurements of Ref. [52], which analyzed the IGRB data and found that they were spatially correlated with galaxy distributions. Compared to the commonly adopted spectral analysis, the tomographic method allows to efficiently extract a dominant IGRB component in certain redshift ranges following galaxy catalogs, as originally proposed for dark matter detection [53–55]. This provides stringent constraints on astrophysical sources [52] and dark matter [56].

We show that the tomographic approach allows to tightly constrain the redshift evolution and the energy spectrum of any class of astrophysical source producing high-energy neutrinos through  $pp$  interactions, especially if the source luminosity density mildly evolves as a function of redshifts. It provides constraints on the expected neutrino flux that are more stringent by up to one order of magnitude with respect to the common spectral approach (e.g., Ref. [47]). We find that any source with a spectrum softer than  $E^{-2.1}$  is excluded, if its redshift evolution is slower than  $(1+z)^3$ . On the other hand, sources with hard spectrum and fast evolution can still be dominant in both gamma-rays and neutrinos.

Besides the  $pp$  origin of the high-energy neutrinos, we assume that: (i) the energy spectrum is a power law,  $E^{-\alpha}$ , extending up to PeV energies; (ii) the source luminosity density evolves as  $(1+z)^\delta$  up to  $z_c$ , and is constant for  $z > z_c$ ; and (iii) the astrophysical sources trace the underlying dark matter distribution. The third assumption is generic for any known extragalactic source that is likely associated with large cosmic structures. We adopt cosmological parameters from Ref. [57].

*Gamma-ray intensity.*—We first introduce a differential gamma-ray intensity,  $I_\gamma(E)$ , as the number of gamma-ray photons received per unit area, unit time, unit solid angle, and unit energy. It is computed as an integral of the gamma-ray window function,  $W_\gamma(E, z)$ ,

over the comoving distance  $\chi$ :

$$I_\gamma(E) = \int d\chi W_\gamma(E, z), \quad (1)$$

$$W_\gamma(E, z) = \frac{1}{4\pi\Lambda E_{\min}'^2} \left( \frac{E}{E_{\min}'} \right)^{-\alpha} \frac{n(z)\langle L_\gamma(z) \rangle}{(1+z)^\alpha} e^{-\tau(E, z)}, \quad (2)$$

where  $n(z)$  is the source number density at  $z$ ,  $\langle L_\gamma(z) \rangle$  is the mean gamma-ray luminosity emitted between  $E_{\min}' = 0.1$  GeV and  $E_{\max}' = 100$  GeV in the source rest frame (as represented by  $'$ ), and

$$\Lambda = \begin{cases} \frac{1 - (E_{\max}'/E_{\min}')^{2-\alpha}}{\alpha-2} & \text{for } \alpha \neq 2, \\ \ln(E_{\max}'/E_{\min}') & \text{for } \alpha = 2. \end{cases} \quad (3)$$

The source luminosity density is assumed to evolve as

$$n(z)\langle L_\gamma(z) \rangle = \mathcal{E}_{\gamma,0} \times \begin{cases} (1+z)^\delta & \text{for } z \leq z_c, \\ (1+z_c)^\delta & \text{for } z > z_c. \end{cases} \quad (4)$$

The constant evolution above  $z_c$  is motivated by the observations of infrared luminosity density of star-forming galaxies (e.g., [58]). We note that unless the redshift dependence continues to increase steeply up to high  $z$ , our conclusions are largely unaffected. Very-high-energy gamma rays are subject to absorption by the extragalactic background light (EBL). This is taken into account through the exponential term in Eq. (2), where  $\tau(E, z)$  is the optical depth [59].

For each set of  $(\alpha, \delta, z_c)$ , by taking  $\mathcal{E}_{\gamma,0}$  as a free parameter, we compute the  $\chi^2$  statistic as follows:

$$\chi^2 = \sum_i \left( \frac{I_{i,\text{dat}} - I_{i,\text{th}}(\mathcal{E}_{\gamma,0}|\alpha, \delta, z_c)}{\sigma_{i,\text{dat}}} \right)^2, \quad (5)$$

where  $I_{i,\text{dat}}$  and  $\sigma_{i,\text{dat}}$  are the spectral intensity data and the associated root-mean-square error in the  $i$ -th energy bin, respectively, and  $I_{i,\text{th}}(\mathcal{E}_{\gamma,0})$  is the theoretical model intensity for  $\mathcal{E}_{\gamma,0}$ . The 95% confidence level (CL) upper limit on  $\mathcal{E}_{\gamma,0}$  is obtained by solving  $\Delta\chi^2 = \chi^2 - \chi_{\min}^2 = 2.71$ .

The top panel of Fig. 1 shows the gamma-ray spectrum for  $\alpha = 2.2$ ,  $\delta = 2$ , and  $z_c = 1.5$  (blue dotted), compared with the IGRB measured by Fermi [48]. The value of the local luminosity density  $\mathcal{E}_{\gamma,0}$  corresponding to the 95% CL upper limit is  $\mathcal{E}_{\gamma,0}^{95\% \text{ CL}} = 2.5 \times 10^{45}$  erg yr $^{-1}$  Mpc $^{-1}$ .

*Cross correlation with galaxy catalogs.*—The cross-correlation angular power spectrum,  $C_\ell^{\gamma g}$ , between the gamma-ray intensity,  $I_\gamma(\hat{n})$ , and the galaxy surface density,  $\Sigma_g(\hat{n})$ , is related to the angular correlation function through the following relation (e.g., [54]):

$$\langle \delta I_\gamma(\hat{n}) \delta \Sigma_g(\hat{n} + \theta) \rangle = \sum_\ell \frac{2\ell + 1}{4\pi} C_\ell^{\gamma g} \mathcal{W}_\ell P_\ell(\cos \theta), \quad (6)$$

where  $\delta I_\gamma = I_\gamma - \langle I_\gamma \rangle$ ,  $\delta \Sigma_g = \Sigma_g - \langle \Sigma_g \rangle$ ,  $P_\ell(\cos \theta)$  is the Legendre polynomial, and  $\mathcal{W}_\ell$  is the beam window

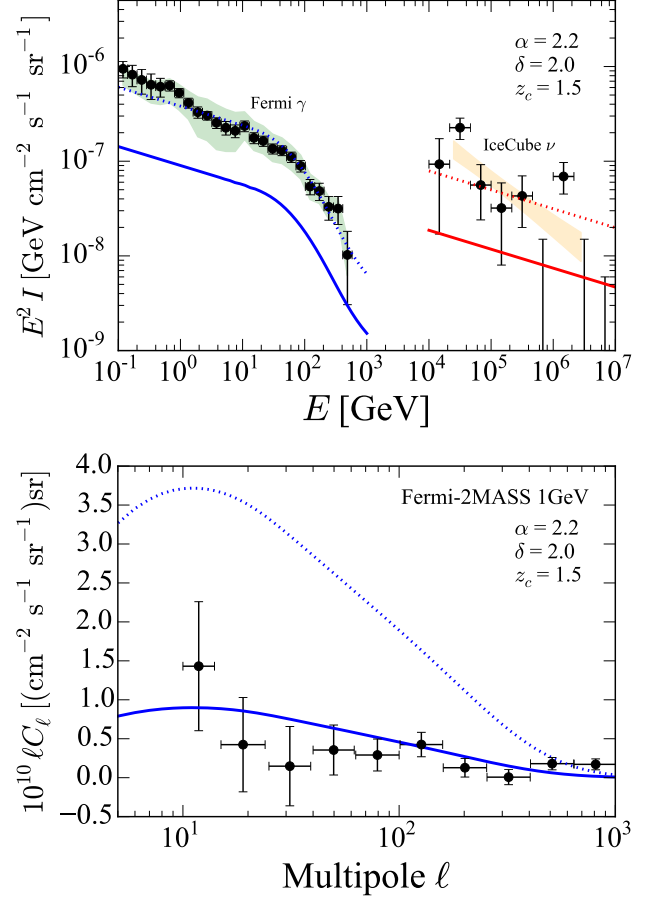


FIG. 1. *Top:* Gamma-ray (blue) and neutrino (red) intensities for a model with  $\alpha = 2.2$ ,  $\delta = 2$ , and  $z_c = 1.5$ . The dotted curves correspond to the 95% CL upper limit due to the Fermi spectrum data (the green band represents the systematic uncertainty due to the subtraction of the Galactic emission [48]). The solid curves correspond to the same limit but due to the cross-correlation data. IceCube data for the neutrino intensity are shown above 10 TeV, whereas the orange band represents the 68% CL region of the corresponding best-fit single power-law model [5]. *Bottom:* Cross-correlation angular power spectrum between the Fermi data, above 1 GeV, and the 2MASS galaxies, compared with the measurements by Ref. [52]. Model parameters as well as line types are the same as the top panel.

function (i.e., the Legendre transform of the point spread function of the Fermi-LAT [52]).

The angular cross-power spectrum  $C_\ell^{\gamma g}$  is computed as (e.g., [54])

$$C_\ell^{\gamma g} = \int \frac{d\chi}{\chi^2} W_\gamma(z) W_g(z) P_{\gamma g} \left( k = \frac{\ell}{\chi}, z \right), \quad (7)$$

where  $W_\gamma(z)$  is the integrated gamma-ray window function, and  $W_g(z)$  is the galaxy window function that is related to the galaxy redshift distribution,  $dN_g/dz$ , via  $W_g(z) = (d \ln N_g / dz)(dz / d\chi)$ . We approximate the

cross-correlation power spectrum between the gamma-ray emitters and the galaxy catalogs as  $P_{\gamma g} \approx b_{\gamma} b_g P_m$ , where  $P_m$  is the nonlinear matter power spectrum computed with the publicly available CLASS code [60], and  $b_g$  and  $b_{\gamma}$  are the bias factors for the catalog galaxies and the gamma-ray emitters, respectively. We assume that gamma-ray sources are unbiased tracers of the dark matter distribution, i.e.,  $b_{\gamma} = 1$ . Since astrophysical sources are typically positively biased dark matter tracers (e.g., [52] and references therein), it is a conservative assumption.

The cross-correlation analysis of Ref. [52] adopted five different catalogs: Two Micron All Sky Survey (2MASS), quasars in the Sloan Digital Sky Survey (SDSS), the SDSS main galaxy sample, luminous red galaxies in SDSS, and radio galaxies in the NRAO VLA Sky Survey (NVSS). Each of these catalogs traces underlying dark matter distribution in a certain redshift range with a characteristic bias  $b_g$  as in Ref. [52]. Although some of them represent AGNs, they can be used the same way as galaxies, for which we call them “galaxy” catalogs collectively. We use a redshift distribution  $dN_g/dz$  and a typical bias  $b_g$  appropriate for each catalog, and three different energy ranges for the gamma rays ( $> 500$  MeV,  $> 1$  GeV, and  $> 10$  GeV) [52].

Similarly to the spectral analysis, for each given set of  $(\alpha, \delta, z_c)$ , we compute the  $\chi^2$  as follows:

$$\chi^2 = \sum_{\gamma, g} \sum_{\ell, \ell'} (C_{\text{dat}}^{\gamma g} - C_{\text{th}}^{\gamma g})_{\ell} (\text{Cov}^{-1})_{\ell \ell'} (C_{\text{dat}}^{\gamma g} - C_{\text{th}}^{\gamma g})_{\ell'}, \quad (8)$$

where  $\gamma$  and  $g$  run through three energy bins and five galaxy catalogs, respectively,  $\ell$  and  $\ell'$  represent the multipole bins of the measurements, and  $\text{Cov}$  is the covariance matrix. We again use  $\Delta\chi^2 = 2.71$  as a criterion to obtain the 95% CL upper limit on  $\mathcal{E}_{\gamma,0}$ .

In the bottom panel of Fig. 1, we show, with a solid curve, the  $C_{\ell}^{\gamma g}$  corresponding to the 95% CL upper limit for  $\alpha = 2.2$ ,  $\delta = 2$ , and  $z_c = 1.5$ , compared with the cross-correlation data between the  $> 1$  GeV photons and the 2MASS galaxies, which gives the major contribution to the  $\chi^2$ . The dotted curve, in contrast, is the 95% CL upper limit due to the spectral data alone, and it is clearly inconsistent with the cross-correlation measurement. The top panel of the same figure shows the corresponding energy spectra for both approaches. It is clear that the source with the parameters adopted in Fig. 1 cannot be the main component of the IGRB spectrum because the cross correlation provides a tighter constraint:  $\mathcal{E}_{\gamma,0}^{95\% \text{ CL}} = 5.9 \times 10^{44} \text{ erg yr}^{-1} \text{ Mpc}^{-3}$ .

Figure 2 shows the 95% CL upper limits on  $\mathcal{E}_{\gamma,0}$  as a function of  $\alpha$ , for  $\delta = 2$  and  $z_c = 1.5$ . For a wide range of spectral indices, the cross-correlation data provide constraints more stringent by up to one order of magnitude than the spectral data. We also find that the difference is larger for smaller  $\delta$ , since the cross correlation con-

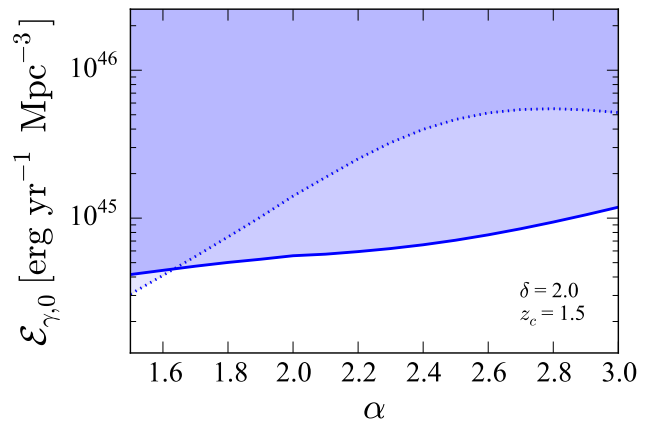


FIG. 2. The 95% CL upper limits on the local gamma-ray luminosity density  $\mathcal{E}_{\gamma,0}$ , between 100 MeV and 100 GeV, as a function of  $\alpha$  for  $\delta = 2$  and  $z_c = 1.5$ . The limits due to spectrum and cross correlation data are shown as dotted and solid curves, respectively.

straints are stronger for smaller redshifts, particularly due to the 2MASS galaxies. For  $\delta \gtrsim 4$ , we find that both the spectrum and cross correlations provide comparable constraints on  $\mathcal{E}_{\gamma,0}$ . The dependence on  $z_c$ , on the other hand, is significantly weaker as long as  $z_c \geq 1$ .

We note that, to be conservative, we did not include secondary gamma rays that are generated by electromagnetic cascades, which would improve the spectral constraints [47]. If the intergalactic magnetic fields are sufficiently weak such that the cascades do not produce halos or larger diffuse emission (e.g., [61]), the tomographic constraints will be also improved by the same factor.

*Constraints on high-energy neutrinos.*—If neutrinos are produced by cosmic ray protons via  $pp$  interactions, their intensity is related to that of gamma rays [62]:

$$I_{\nu}(E_{\nu}) \approx 6 I_{\gamma, \text{no-EBL}}(E_{\gamma}), \quad (9)$$

with  $E_{\gamma} = 2 E_{\nu}$ . Here,  $I_{\nu}$  is the neutrino intensity for *all* flavors, and  $I_{\gamma, \text{no-EBL}}$  is the gamma-ray intensity without EBL absorption. Therefore, constraints on  $I_{\gamma}(E_{\gamma})$  (or  $\mathcal{E}_{\gamma,0}$ ), for each set of the parameters  $(\alpha, \delta, z_c)$ , can be directly transformed into those of a neutrino intensity in the TeV–PeV energy range through Eq. (9).

The top panel of Fig. 1 shows the 95% CL upper limits on  $I_{\nu}(E_{\nu})$  from the IGRB spectrum (red dotted) and the cross-correlation data (red solid) for  $\alpha = 2.2$ ,  $\delta = 2$ , and  $z_c = 1.5$ . We find that while the IGRB spectrum analysis suggests this particular model to be compatible with the IceCube data, the tomographic approach constrains it as a subdominant source.

Figure 3 shows the dependence of the neutrino intensity integrated above 25 TeV on  $\alpha$  and  $\delta$  for a fixed  $z_c = 1.5$ . The intensity range preferred by the best-fit single power-law model of the IceCube data [5] is also

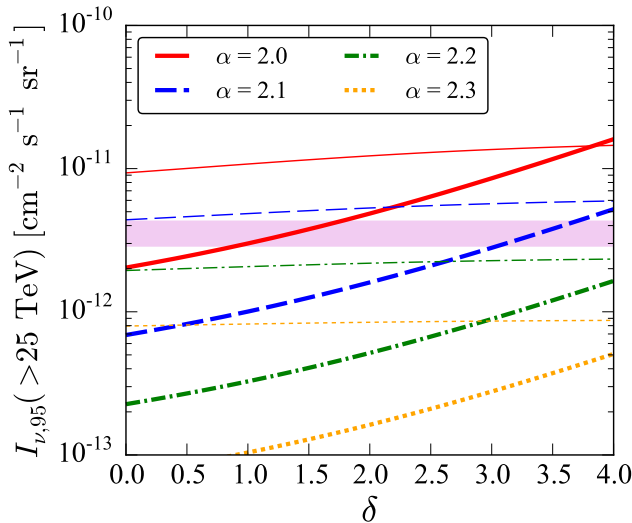


FIG. 3. The 95% CL upper limits on the neutrino intensity integrated above 25 TeV as a function of  $\delta$  for various values of  $\alpha$  and fixed  $z_c = 1.5$ . Thick and thin curves show the limits due to the tomographic and spectral analyses of the IGRB, respectively. The horizontal magenta band shows the 68% CL interval of the best-fit single power-law model for the IceCube neutrino data [5], corresponding to the neutrino band shown in Fig. 1.

shown for comparison. For each model characterized by  $(\alpha, \delta)$ , we show constraints due to the spectral and tomographic data, as thin and thick curves, respectively. Note that the tomographic analysis gives tighter constraints by up to one order of magnitude with respect to the spectral analysis, especially for small  $\delta$ . In particular, for any source class slowly evolving (e.g.,  $\delta \lesssim 3$ ), even a very hard spectrum such as  $E^{-2.1}$  is nearly excluded as dominant source for the IceCube neutrinos. Any soft source with  $\alpha \gtrsim 2.2$  should contribute much less to the total neutrino flux than previously expected (e.g., Refs. [24, 47]). Models with spectrum as hard as  $E^{-2}$ , on the other hand, are still compatible with the IceCube flux level.

*Discussion and outlook.*—Under the hypothesis that the TeV–PeV IceCube neutrinos are mostly generated from  $pp$  interactions in a single astrophysical source class (or more classes with similar properties), Fig. 3 implies that a model with  $\alpha \approx 2.15$  and  $\delta \approx 4$  (for  $z_c = 1.5$ ) can explain most of the neutrino flux. At the same time, sources of this kind can explain most of the IGRB flux as well as the measured cross correlations. We note that in order for such a hard spectrum to be compatible with the IceCube data, a PeV spectral cutoff is required [5] (but data in the northern hemisphere still allow it without a cutoff [6]). Otherwise, the comparison of the current data set with our results might suggest a mixed  $pp$ – $p\gamma$ , or even a pure  $p\gamma$  origin of the IceCube neutrino events.

Interestingly, starburst galaxies well satisfy the above

conditions for the  $pp$  origin, although efficient cosmic ray confinement needs to be achieved [19, 24, 28]. While direct gamma-ray measurements of the redshift evolution of star-forming galaxies are not yet available, observations of their infrared luminosity (or of the star-formation rate) support such steep evolution. In particular, the evolution of starburst galaxies is characterized by  $\delta \gtrsim 4$  up to  $z_c \approx 1.5$  [58]. Here, we assumed that the local correlation between infrared and gamma-ray luminosities [63] holds also at high redshifts.

Based on a modeling of resolved gamma-ray sources, Ref. [64] argued that about 20–30% of the IGRB above 100 MeV can be explained by blazars (a subclass of AGNs). Furthermore, for energies above  $\sim 100$  GeV, the blazar contribution can be substantial, explaining most of the IGRB data and leaving little room for any other source. This might point toward an even harder source population with steep redshift evolution for the neutrinos, which would be, however, subdominant both in the IGRB flux and cross correlations. For example, in the case of  $\alpha = 2$  and  $\delta = 4$ , once we tune the gamma-ray luminosity density to match the level of  $\sim 10\%$  of the IGRB flux and cross correlations, the same model could explain most of the neutrino data.

Clusters and groups of galaxies have also been investigated as potential neutrino sources [40, 47], where cosmic rays, generated through large-scale-structure shocks [37, 40] or injected by star-forming galaxies [27], interact with the intracluster medium. Since the cluster/group number density decreases as a function of redshift, implying a small value of  $\delta$ , tomographic constraints are very stringent. When considering starbursts or AGNs in clusters/groups, their quick redshift evolution has to be coupled with the negative one of clusters. As an example, we calculated that the overall evolution is locally characterized by  $\delta < 2$  that quickly decreases to negative values for  $z \gtrsim 0.5$ . In addition, clusters are largely biased with respect to dark matter (i.e.,  $b_\gamma \sim 5$  for  $10^{15} M_\odot$  and  $z = 0$  [65]), making the tomographic constraints tighter than those shown in Fig. 3. Therefore, clusters and groups are disfavored by the cross-correlation data.

These arguments cannot be applied to  $p\gamma$  sources, such as AGNs [12, 13, 15, 16, 18]. This is because the threshold for  $p\gamma$  interactions is typically very high. It is also argued that such sources may be optically thick for GeV gamma rays [66]. In any case, it appears difficult that AGNs can be responsible for all the IceCube neutrino events. In fact, Ref. [18] recently suggested that the diffuse emission from blazars can explain the IceCube neutrino flux at energies above  $\sim$ PeV only.

In conclusion, the tomographic method that we apply for the first time to high-energy neutrinos yields tight constraints on the properties of any hadronuclear source, providing complementary bounds on their injection spectral index and redshift evolution. In particular, we show that only hard spectrum sources with fast redshift evolu-

tion can produce a neutrino flux at the same level as the IceCube measurement. The potential relevance of this method in connection with high-energy neutrinos is expected to quickly increase in the near future, because of the growing galaxy samples for the cross-correlation analysis, including cosmic shear measurements that already seem promising [67–69].

We thank Alessandro Cuoco for sharing the cross-correlation data and their covariance matrices presented in Ref. [52] and for comments on the manuscript, and Kohta Murase for discussions. This work was supported by the Netherlands Organization for Scientific Research (NWO) through Vidi (SA and IT) and Veni (FZ) Grants.

- 
- [1] M. G. Aartsen *et al.* (IceCube), Phys. Rev. Lett. **111**, 021103 (2013), arXiv:1304.5356 [astro-ph.HE].
  - [2] M. G. Aartsen *et al.* (IceCube), Science **342**, 1242856 (2013), arXiv:1311.5238 [astro-ph.HE].
  - [3] M. G. Aartsen *et al.* (IceCube), Phys. Rev. Lett. **113**, 101101 (2014), arXiv:1405.5303 [astro-ph.HE].
  - [4] M. G. Aartsen *et al.* (IceCube), Phys. Rev. D **91**, 022001 (2015), arXiv:1410.1749 [astro-ph.HE].
  - [5] M. G. Aartsen *et al.* (IceCube), Astrophys. J. **809**, 98 (2015), arXiv:1507.03991 [astro-ph.HE].
  - [6] M. G. Aartsen *et al.* (IceCube), Phys. Rev. Lett. **115**, 081102 (2015), arXiv:1507.04005 [astro-ph.HE].
  - [7] L. A. Anchordoqui *et al.*, JHEAp **1-2**, 1 (2014), arXiv:1312.6587 [astro-ph.HE].
  - [8] E. Waxman, in *Rencontres du Vietnam: Windows on the Universe Quy Nhon, Binh Dinh, Vietnam, August 11-17, 2013* (2013) arXiv:1312.0558 [astro-ph.HE].
  - [9] F. W. Stecker, C. Done, M. H. Salamon, and P. Sommers, Phys. Rev. Lett. **66**, 2697 (1991), [Erratum: Phys. Rev. Lett. 69, 2738 (1992)].
  - [10] F. W. Stecker, Phys. Rev. D **72**, 107301 (2005), arXiv:astro-ph/0510537 [astro-ph].
  - [11] O. E. Kalashev, A. Kusenko, and W. Essey, Phys. Rev. Lett. **111**, 041103 (2013), arXiv:1303.0300 [astro-ph.HE].
  - [12] F. W. Stecker, Phys. Rev. D **88**, 047301 (2013), arXiv:1305.7404 [astro-ph.HE].
  - [13] K. Murase, Y. Inoue, and C. D. Dermer, Phys. Rev. D **90**, 023007 (2014), arXiv:1403.4089 [astro-ph.HE].
  - [14] S. S. Kimura, K. Murase, and K. Toma, Astrophys. J. **806**, 159 (2015), arXiv:1411.3588 [astro-ph.HE].
  - [15] C. D. Dermer, K. Murase, and Y. Inoue, JHEAp **3-4**, 29 (2014), arXiv:1406.2633 [astro-ph.HE].
  - [16] O. Kalashev, D. Semikoz, and I. Tkachev, (2014), arXiv:1410.8124 [astro-ph.HE].
  - [17] B. Khiali and E. M. d. G. D. Pino, (2015), arXiv:1506.01063 [astro-ph.HE].
  - [18] P. Padovani, M. Petropoulou, P. Giommi, and E. Resconi, Mon. Not. R. Astron. Soc. **452**, 1877 (2015), arXiv:1506.09135 [astro-ph.HE].
  - [19] A. Loeb and E. Waxman, JCAP **0605**, 003 (2006), arXiv:astro-ph/0601695 [astro-ph].
  - [20] T. A. Thompson, E. Quataert, E. Waxman, and A. Loeb, (2006), arXiv:astro-ph/0608699 [astro-ph].
  - [21] H.-N. He, T. Wang, Y.-Z. Fan, S.-M. Liu, and D.-M. Wei, Phys. Rev. D **87**, 063011 (2013), arXiv:1303.1253 [astro-ph.HE].
  - [22] R.-Y. Liu, X.-Y. Wang, S. Inoue, R. Crocker, and F. Aharonian, Phys. Rev. D **89**, 083004 (2014), arXiv:1310.1263 [astro-ph.HE].
  - [23] X.-C. Chang and X.-Y. Wang, Astrophys. J. **793**, 131 (2014), arXiv:1406.1099 [astro-ph.HE].
  - [24] I. Tamborra, S. Ando, and K. Murase, JCAP **1409**, 043 (2014), arXiv:1404.1189 [astro-ph.HE].
  - [25] L. A. Anchordoqui, T. C. Paul, L. H. M. da Silva, D. F. Torres, and B. J. Vlcek, Phys. Rev. D **89**, 127304 (2014), arXiv:1405.7648 [astro-ph.HE].
  - [26] S. Chakraborty and I. Izaguirre, Phys. Lett. B **745**, 35 (2015), arXiv:1501.02615 [hep-ph].
  - [27] N. Senno, P. Mészáros, K. Murase, P. Baerwald, and M. J. Rees, Astrophys. J. **806**, 24 (2015), arXiv:1501.04934 [astro-ph.HE].
  - [28] I. Bartos and S. Marka, (2015), arXiv:1509.00983 [astro-ph.HE].
  - [29] E. Waxman and J. N. Bahcall, Phys. Rev. D **59**, 023002 (1999), arXiv:hep-ph/9807282 [hep-ph].
  - [30] P. Mészáros and E. Waxman, Phys. Rev. Lett. **87**, 171102 (2001), arXiv:astro-ph/0103275 [astro-ph].
  - [31] K. Murase and S. Nagataki, Phys. Rev. D **73**, 063002 (2006), arXiv:astro-ph/0512275 [astro-ph].
  - [32] N. Gupta and B. Zhang, Astropart. Phys. **27**, 386 (2007), arXiv:astro-ph/0606744 [astro-ph].
  - [33] K. Murase, K. Ioka, S. Nagataki, and T. Nakamura, Astrophys. J. **651**, L5 (2006), arXiv:astro-ph/0607104 [astro-ph].
  - [34] R.-Y. Liu and X.-Y. Wang, Astrophys. J. **766**, 73 (2013), arXiv:1212.1260 [astro-ph.HE].
  - [35] K. Murase and K. Ioka, Phys. Rev. Lett. **111**, 121102 (2013), arXiv:1306.2274 [astro-ph.HE].
  - [36] I. Tamborra and S. Ando, (2015), arXiv:1504.00107 [astro-ph.HE].
  - [37] K. Murase, S. Inoue, and S. Nagataki, Astrophys. J. **689**, L105 (2008), arXiv:0805.0104 [astro-ph].
  - [38] K. Kotera, D. Allard, K. Murase, J. Aoi, Y. Dubois, T. Pierog, and S. Nagataki, Astrophys. J. **707**, 370 (2009), arXiv:0907.2433 [astro-ph.HE].
  - [39] K. Murase and J. F. Beacom, JCAP **1302**, 028 (2013), arXiv:1209.0225 [astro-ph.HE].
  - [40] F. Zandanel, I. Tamborra, S. Gabici, and S. Ando, Astron. Astrophys. **578**, A32 (2015), arXiv:1410.8697 [astro-ph.HE].
  - [41] B. Feldstein, A. Kusenko, S. Matsumoto, and T. T. Yanagida, Phys. Rev. D **88**, 015004 (2013), arXiv:1303.7320 [hep-ph].
  - [42] A. Esmaili and P. D. Serpico, JCAP **1311**, 054 (2013), arXiv:1308.1105 [hep-ph].
  - [43] A. Esmaili, S. K. Kang, and P. D. Serpico, JCAP **1412**, 054 (2014), arXiv:1410.5979 [hep-ph].
  - [44] J. Zavala, Phys. Rev. D **89**, 123516 (2014), arXiv:1404.2932 [astro-ph.HE].
  - [45] K. Murase, R. Laha, S. Ando, and M. Ahlers, Phys. Rev. Lett. **115**, 071301 (2015), arXiv:1503.04663 [hep-ph].
  - [46] W. Winter, Phys. Rev. D **88**, 083007 (2013), arXiv:1307.2793 [astro-ph.HE].
  - [47] K. Murase, M. Ahlers, and B. C. Lacki, Phys. Rev. D **88**, 121301 (2013), arXiv:1306.3417 [astro-ph.HE].
  - [48] M. Ackermann *et al.* (Fermi-LAT), Astrophys. J. **799**, 86 (2015), arXiv:1410.3696 [astro-ph.HE].
  - [49] L. A. Anchordoqui, H. Goldberg, M. H. Lynch, A. V. Olinto, T. C. Paul, and T. J. Weiler, Phys. Rev. D **89**,

- 083003 (2014), arXiv:1306.5021 [astro-ph.HE].
- [50] K. Fang, T. Fujii, T. Linden, and A. V. Olinto, *Astrophys. J.* **794**, 126 (2014), arXiv:1404.6237 [astro-ph.HE].
  - [51] M. D. Kistler, T. Stanev, and H. Yüksel, *Phys. Rev. D* **90**, 123006 (2014), arXiv:1301.1703 [astro-ph.HE].
  - [52] J.-Q. Xia, A. Cuoco, E. Branchini, and M. Viel, *Astrophys. J. Suppl.* **217**, 15 (2015), arXiv:1503.05918 [astro-ph.CO].
  - [53] S. Ando, A. Benoit-Lévy, and E. Komatsu, *Phys. Rev. D* **90**, 023514 (2014), arXiv:1312.4403 [astro-ph.CO].
  - [54] S. Ando, *JCAP* **1410**, 061 (2014), arXiv:1407.8502 [astro-ph.CO].
  - [55] N. Fornengo and M. Regis, *Front. Physics* **2**, 6 (2014), arXiv:1312.4835 [astro-ph.CO].
  - [56] A. Cuoco, J.-Q. Xia, M. Regis, E. Branchini, N. Fornengo, and M. Viel, (2015), arXiv:1506.01030 [astro-ph.HE].
  - [57] P. A. R. Ade *et al.* (Planck), (2015), arXiv:1502.01589 [astro-ph.CO].
  - [58] C. Gruppioni *et al.*, *Mon. Not. R. Astron. Soc.* **432**, 23 (2013), arXiv:1302.5209 [astro-ph.CO].
  - [59] J. D. Finke, S. Razzaque, and C. D. Dermer, *Astrophys. J.* **712**, 238 (2010), arXiv:0905.1115 [astro-ph.HE].
  - [60] D. Blas, J. Lesgourgues, and T. Tram, *JCAP* **1107**, 034 (2011), arXiv:1104.2933 [astro-ph.CO].
  - [61] S. Ando and A. Kusenko, *Astrophys. J.* **722**, L39 (2010), arXiv:1005.1924 [astro-ph.HE].
  - [62] L. A. Anchordoqui, H. Goldberg, F. Halzen, and T. J. Weiler, *Phys. Lett. B* **600**, 202 (2004), arXiv:astro-ph/0404387 [astro-ph].
  - [63] M. Ackermann *et al.* (Fermi-LAT), *Astrophys. J.* **755**, 164 (2012), arXiv:1206.1346 [astro-ph.HE].
  - [64] M. Ajello *et al.*, *Astrophys. J.* **800**, L27 (2015), arXiv:1501.05301 [astro-ph.HE].
  - [65] J. L. Tinker, B. E. Robertson, A. V. Kravtsov, A. Klypin, M. S. Warren, G. Yepes, and S. Gottlober, *Astrophys. J.* **724**, 878 (2010), arXiv:1001.3162 [astro-ph.CO].
  - [66] K. Murase, D. Guetta, and M. Ahlers, (2015), arXiv:1509.00805 [astro-ph.HE].
  - [67] S. Camera, M. Fornasa, N. Fornengo, and M. Regis, *JCAP* **1506**, 029 (2015), arXiv:1411.4651 [astro-ph.CO].
  - [68] M. Shirasaki, S. Horiuchi, and N. Yoshida, *Phys. Rev. D* **90**, 063502 (2014), arXiv:1404.5503 [astro-ph.CO].
  - [69] N. Fornengo, L. Perotto, M. Regis, and S. Camera, *Astrophys. J.* **802**, L1 (2015), arXiv:1410.4997 [astro-ph.CO].